



King Saud University
Arabian Journal of Chemistry

www.ksu.edu.sa
www.sciencedirect.com



ORIGINAL ARTICLE

Effect of silica coating on Fe₃O₄ magnetic nanoparticles for lipase immobilization and their application for biodiesel production

Baskar Thangaraj, Zhaohua Jia, Lingmei Dai, Dehua Liu, Wei Du *

Institute of Applied Chemistry, Department of Chemical Engineering, Tsinghua University, Beijing 100084, PR China

Received 17 June 2016; accepted 4 September 2016

KEYWORDS

Magnetic nanoparticles;
Organosilane;
Functionalization;
Covalent binding;
Lipase immobilization;
Transesterification;
Biodiesel

Abstract The scope of this study was to prepare different organosilane-modified Fe₃O₄@SiO₂ core magnetic nanocomposites with immobilized lipase and explore their potential application in biodiesel field. Fe₃O₄ magnetic nanoparticles prepared by co-precipitation method were coated with various ratios of SiO₂ as per Stöber method and further functionalized by different organosilane compounds APTES (3-aminopropyltriethoxysilane) and MPTMS (3-mercaptopropyltrimethoxysilane). Functionalized Fe₃O₄@SiO₂ magnetic nanoparticles were immobilized with free lipase NS81006 by glutaraldehyde cross-linking reagent. The functional groups, structure, morphology and magnetic susceptibility of synthesized and modified Fe₃O₄@SiO₂ magnetic nanoparticles were characterized by FTIR, XRD, SEM, TEM, and VSM techniques. The immobilization efficiency and activity recovery were reduced by increasing the ratio of silica coating on Fe₃O₄. Maximum activity recovery (84% by APTES, 83% by MPTMS) and biodiesel yield (>90%) were obtained by lipase immobilized on Fe₃O₄@SiO₂ support when the Fe₃O₄ and SiO₂ (TEOS) ratio was low (1:0.25).

© 2016 The Authors. Production and hosting by Elsevier B.V. on behalf of King Saud University. This is an open access article under the CC BY-NC-ND license (<http://creativecommons.org/licenses/by-nc-nd/4.0/>).

1. Introduction

Biodiesel has become a very attractive fuel option because of its environmental benefits characterized by lower combustion emission of carbon monoxide, and particulate matter and sulfur compounds besides the by-products are non-toxic and easily biodegradable (Tao et al.,

2008; Serio et al., 2008; Baskar and Raj, 2013). Biodiesel is the methyl or ethyl esters of fatty acid made from virgin or used edible, non-edible oils and animal fats through transesterification reaction which is richly favored by the involvement of chemical or biological catalysts.

Chemical based catalytic transesterification process is efficient in all aspects, although the process suffers high energy consumption and waste water treatment due to the presence of unreacted chemicals (Shah et al., 2004; Bajaj et al., 2010).

On the other hand enzymatic mode of transesterification discounts many of the disadvantages (Zarei et al., 2014). Major advantages of lipase as a biocatalyst are their chemo-region and stereo specificity as well as soft reaction conditions (Fjerbaek et al., 2009). The lipase catalyzed reaction is often hampered by its lack of long-term stability under process conditions, difficulties in recovery and recycling

* Corresponding author.

E-mail address: duwei@tsinghua.edu.cn (W. Du).

Peer review under responsibility of King Saud University.



<http://dx.doi.org/10.1016/j.arabjc.2016.09.004>

1878-5352 © 2016 The Authors. Production and hosting by Elsevier B.V. on behalf of King Saud University.

This is an open access article under the CC BY-NC-ND license (<http://creativecommons.org/licenses/by-nc-nd/4.0/>).

Please cite this article in press as: Thangaraj, B. et al., Effect of silica coating on Fe₃O₄ magnetic nanoparticles for lipase immobilization and their application for biodiesel production 3O₄ magnetic nanoparticles →. Arabian Journal of Chemistry (2016), <http://dx.doi.org/10.1016/j.arabjc.2016.09.004>

(Kumari et al., 2009; Bajaj et al., 2010) and its cost intensiveness. Such problems can be overcome by immobilization, which enhances stability and easy separation from the reaction mixture. Non-magnetic materials were successfully employed and were functioning on adsorption route (Macario et al., 2008; Palomo et al., 2002).

Lipase immobilized on magnetic nanoparticles as carrier is known to offer high specific surface area which favors the binding efficiency, minimize mass transfer resistance and fouling, enhance reaction rate and increase turnover number (TON), prevent lipase contamination of the product and improve the economic advantage due to increased cycle (Wang et al., 2012; Siódmiak et al., 2013).

Magnetic nanoparticles (MNPs) are efficient and significant carrier in lipase immobilization (Kumar et al., 2013; Xie and Ma, 2009). Fe_3O_4 and $\gamma\text{-Fe}_2\text{O}_3$ are considered as ideal MNPs due to their biocompatibility, stability, high surface area to volume ratio and superparamagnetic properties (Lu et al., 2007). Besides, naked- Fe_3O_4 MNPs are non-porous materials with high activity and are easily oxidized in atmospheric air affecting the loss of magnetic properties and dispersibility (Wu et al., 2008). The stability of MNPs is reported to be improved by surface functionalization through effective protection strategies (Wei et al., 2006; Bae et al., 2012). Carbon, noble metals, metal oxides, and chitosan are often considered as potential candidates for the surface modification of naked- Fe_3O_4 (Wu et al., 2008). Silica is an inert coating material which is known to prevent the aggregation of the superparamagnetic core in liquid media thereby improving the stability, biodegradability, and biocompatibility and minimizing the toxicity (Kunzmann et al., 2011; Morel et al., 2008). Furthermore, silica layer supplies rich silanol groups that can easily react with organosilane compounds (Ahmadi et al., 2014) and effectively binds with lipase molecules for biocatalytic applications (Ahangaran et al., 2013; Wang et al., 2012).

There are many promising techniques for coating on the surface of the MNPs with silica such as Stöber method, sol-gel process, aerosol pyrolysis (Wu et al., 2008) and micro emulsion (Kunzmann et al., 2011). Among them silica coating by Stöber method is popular (Santra et al., 2001; Lu et al., 2007). Stöber method is characterized by the absence of any surfactant (Rao et al., 2005; Hui et al., 2011).

Ongoing through the published information, it is known that the ratio between the nanoparticles and tetraethyl orthosilicate (TEOS) (w:v) largely plays role on the efficiency of lipase immobilization and activity recovery. Therefore in this work focus is made to assess the impact of the ratio between Fe_3O_4 and TEOS on the immobilization efficiency and activity recovery of lipase NS81006 which was hitherto not worked except an investigation by one of the present authors on the same enzyme without immobilization.

2. Materials and methods

2.1. Materials

(3-aminopropyl) triethoxysilane (APTES), (3-mercaptopropyl) trimethoxysilane (MPTMS) [Sigma-Aldrich], Iron (II) sulfate heptahydrate, iron (II) chloride hexahydrate [Xilong Chemical Co. Ltd, China], Glutaraldehyde (50%) and tetra orthosilicate (TEOS) [Tianjin Jinke Fine Chemical Research Institute, China] required for this study were procured shortly before the commencement of the project. Free lipase (NS81006) from the genetically modified *Aspergillus niger* was provided by Novozymes (Denmark). Tributyrin [Tokyo Chemical Industry, Japan] and Bradford reagent (BCA kit) [Sigma-Aldrich] and other chemicals were used as received without further purification.

2.2. Characterizations

FTIR spectra with a wave number $400\text{--}4000\text{ cm}^{-1}$ were developed through a Thermo Scientific Nicolet iN10 FTIR

microscope (Thermo Nicolet Corporation, Madison, WI) equipped with a liquid nitrogen cooled MCT detector. X-ray diffraction (XRD) patterns were analyzed by XRD-6000 diffractometer (Shimadzu, Japan) using Ni-filtered Cu K α radiation ($\nu = 1.54\text{ \AA}$) at 40 kV and 40 mA. Surface characteristics of MNPs were observed by using scanning electron microscope (SEM) at 15 kV (Hitachi Japan S-3400N II). Images were obtained at the magnification range from $45\times$ to $30,000\times$ depending on the feature to be examined. TEM measurements were made by FEI TECNAI G2 20 (USA) transmission electron microscope at 200 kV. The magnetic properties of the synthesized and modified magnetic materials were characterized with a vibrating sample magnetometer (VSM) using IDEASVSM at room temperature. Synthesized biodiesel (fatty acid methyl esters) was analyzed by Agilent 7890AGC (Agilent Technologies, Santa Clara, USA) equipped with CP-FFAPCB capillary column ($25\text{ m} \times 0.32\text{ mm} \times 0.30\text{ m}$). The heptadecanoic acid methyl ester was used as internal standard. The upper layer and 0.6 mL of 0.7 mg mL^{-1} heptadecanoic acid methyl ester (ethanol as a solvent) were mixed thoroughly. From the resultant mixture $1\text{ }\mu\text{L}$ was taken for analysis. The temperature for injection and Flame ionization detector (FID) was $250\text{ }^\circ\text{C}$. The column temperature was initially maintained at $160\text{ }^\circ\text{C}$ for 0.5 min. Thereafter it was increased to $250\text{ }^\circ\text{C}$ at the rate of $10\text{ }^\circ\text{C min}^{-1}$ and kept at $250\text{ }^\circ\text{C}$ for 6 min.

2.3. Preparation of Fe_3O_4 MNPs

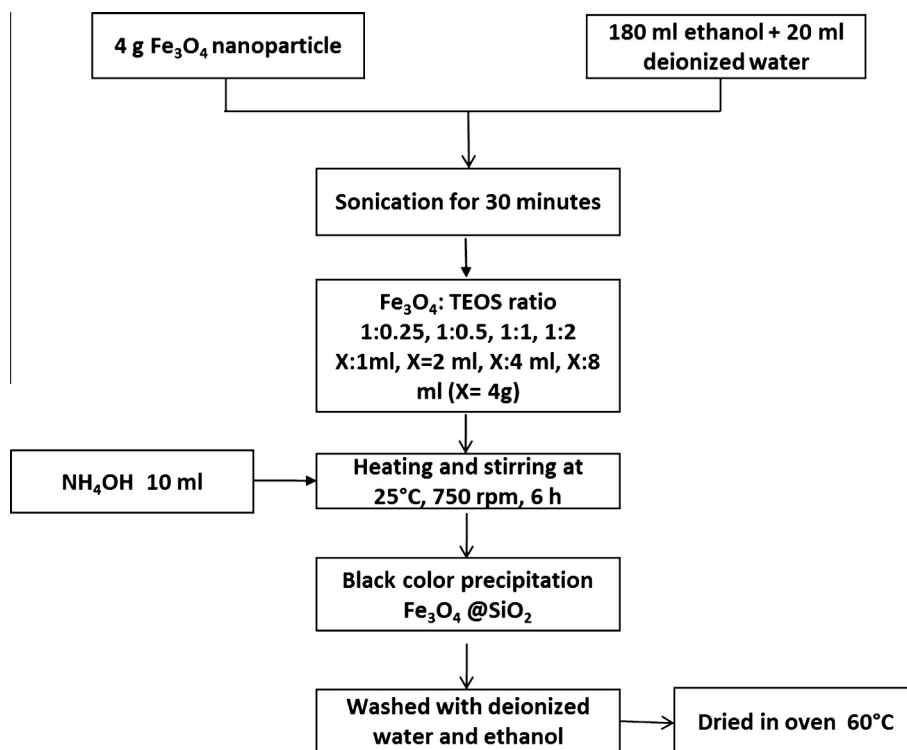
Iron (II) sulfate heptahydrate and iron (II) chloride were dissolved at a molar ratio of 1:2 in 200 mL deionized water and stirred vigorously at $30\text{ }^\circ\text{C}$ for 30 min, while stirring ammonium hydroxide (NH_4OH) (25% in water v/v) was added dropwise to the mixture. The black precipitate Fe_3O_4 emerged was heated at $85\text{ }^\circ\text{C}$ and isolated using a magnetic bar. These particles were then sequentially washed with deionized water and ethanol. The MNPs dried in hot air oven at $70\text{ }^\circ\text{C}$ were preserved in a desiccator for further use.

2.4. Preparation of various ratios of $\text{Fe}_3\text{O}_4@\text{SiO}_2$ core-shell MNPs

Fe_3O_4 (4 g) was dispersed in 180 mL ethanol and 20 mL deionized water by sonication process. To the above TEOS were added and was sonicated well. Dilute ammonium hydroxide (25%) was added slowly dropwise (10 mL) while stirring the reaction mixture. It was then heated at room temperature for 6 h. The product thus obtained ($\text{Fe}_3\text{O}_4@\text{SiO}_2$) was collected by a magnetic bar and was washed well with deionized water and ethanol to remove impurities. Following that they were dried in an oven at $60\text{ }^\circ\text{C}$ and stored in a desiccator for further use. Different quantities of TEOS were incorporated with Fe_3O_4 and used in this study (Scheme 1). The ratio of Fe_3O_4 : TEOS was 1:0.25, 1:0.5, 1:1 and 1:2 (for each 4 g of Fe_3O_4 , 1, 2, 4 and 8 mL of TEOS were used).

2.5. Preparation of APTES and MPTMS-modified $\text{Fe}_3\text{O}_4@\text{SiO}_2$ MNPs

$\text{Fe}_3\text{O}_4@\text{SiO}_2$ MNP (0.5 g) was dispersed in ethanol by ultrasonication for 30 min. To this 0.3 mL APTES was added



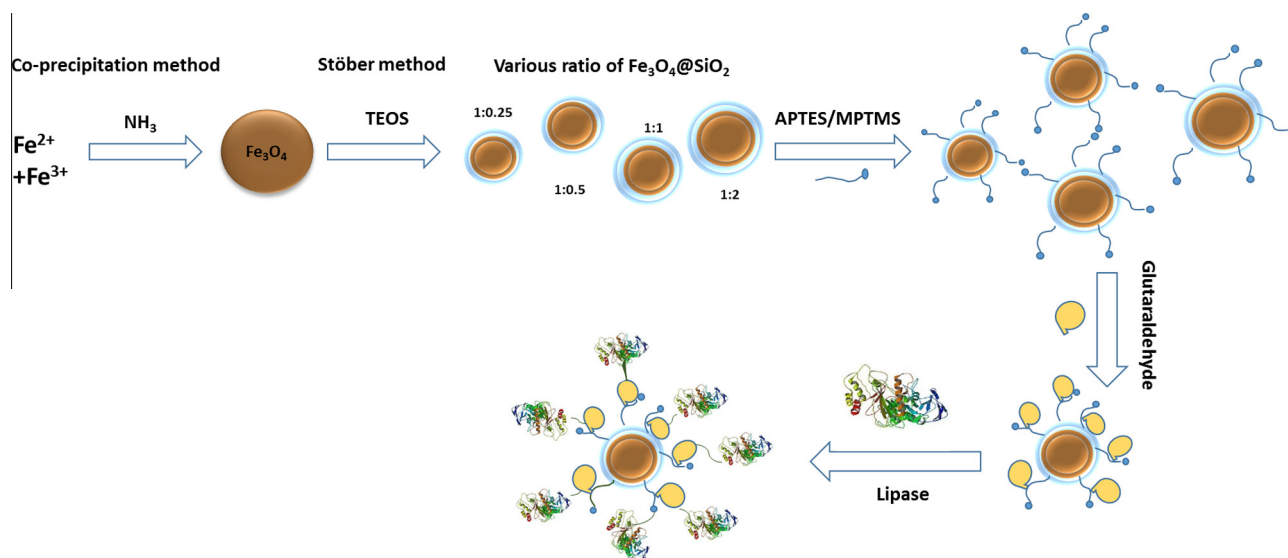
Scheme 1 Schematic diagram of preparing Fe₃O₄@SiO₂ magnetic nanoparticles with different quantities of TEOS.

and sonication continued. The dispersed particles were placed in the shaker at 25 °C. The functionalized-Fe₃O₄@SiO₂ MNPs were collected by a magnetic bar and rinsed with deionized water and ethanol to remove the excess organosilane reagents. In case of MPTMS 0.6 mL was used. [Scheme 2](#) illustrates the pathways of the reaction wherein the transformation sequences and the emergence of products are indicated.

2.6. Lipase immobilization

The functionalized-Fe₃O₄@SiO₂ magnetic nanoparticles thus prepared were treated with 20 mL of glutaraldehyde cross-

linking reagent (10% v/v) for 2 h. Then it was washed thrice with deionized water to free it from unreacted glutaraldehyde. A known amount of lipase and phosphate buffer solution (sodium dihydrogen phosphate at pH – 7.0) was added into the glutaraldehyde treated Fe₃O₄@SiO₂ MNPs. The mixture was vigorously shaken at room temperature for several hours. Thereafter the lipase immobilized Fe₃O₄@SiO₂ MNPs was isolated by applying external magnetic field and was washed with the said buffer solution repeatedly. The supernatant (unbound lipase) solution was measured so as to assess the lipase immobilization efficiency using Bradford and BCA (bicinchoninic acid assay) kit at a wavelength of 562 nm. The



Scheme 2 Organosilane compounds and lipase immobilization on the surface of Fe₃O₄@SiO₂ magnetic nanoparticles.

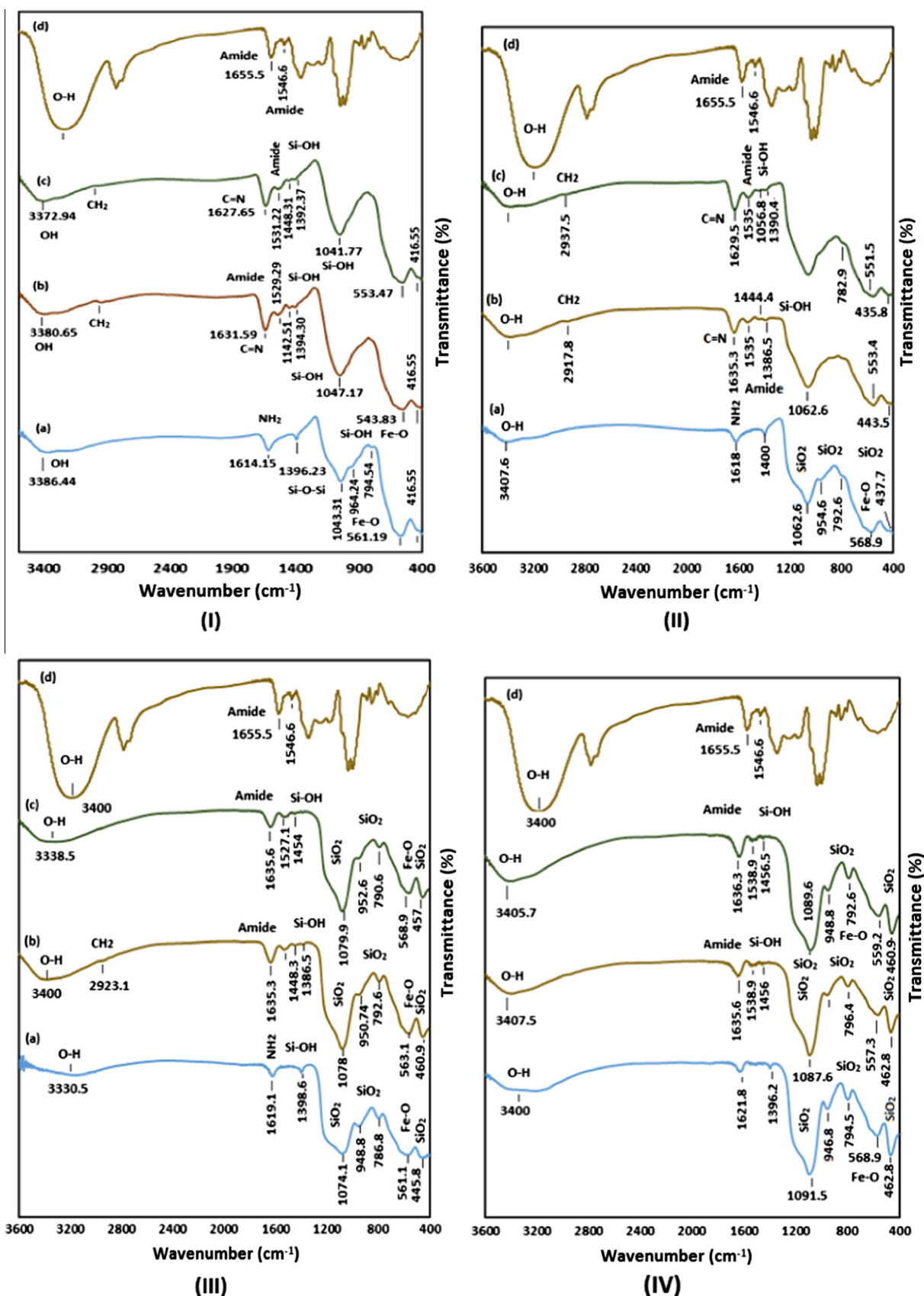


Figure 1 FTIR spectra of Fe₃O₄@SiO₂ developed by incorporating Fe₃O₄ with different ratios of TEOS (I) 1:0.25, (II) 1:0.5, (III) 1:1 and (IV) 1:2. (a) Fe₃O₄@SiO₂, (b) lipase immobilized on APTES-Fe₃O₄@SiO₂, (c) lipase immobilized on MPTMS-Fe₃O₄@SiO₂ and (d) pure lipase.

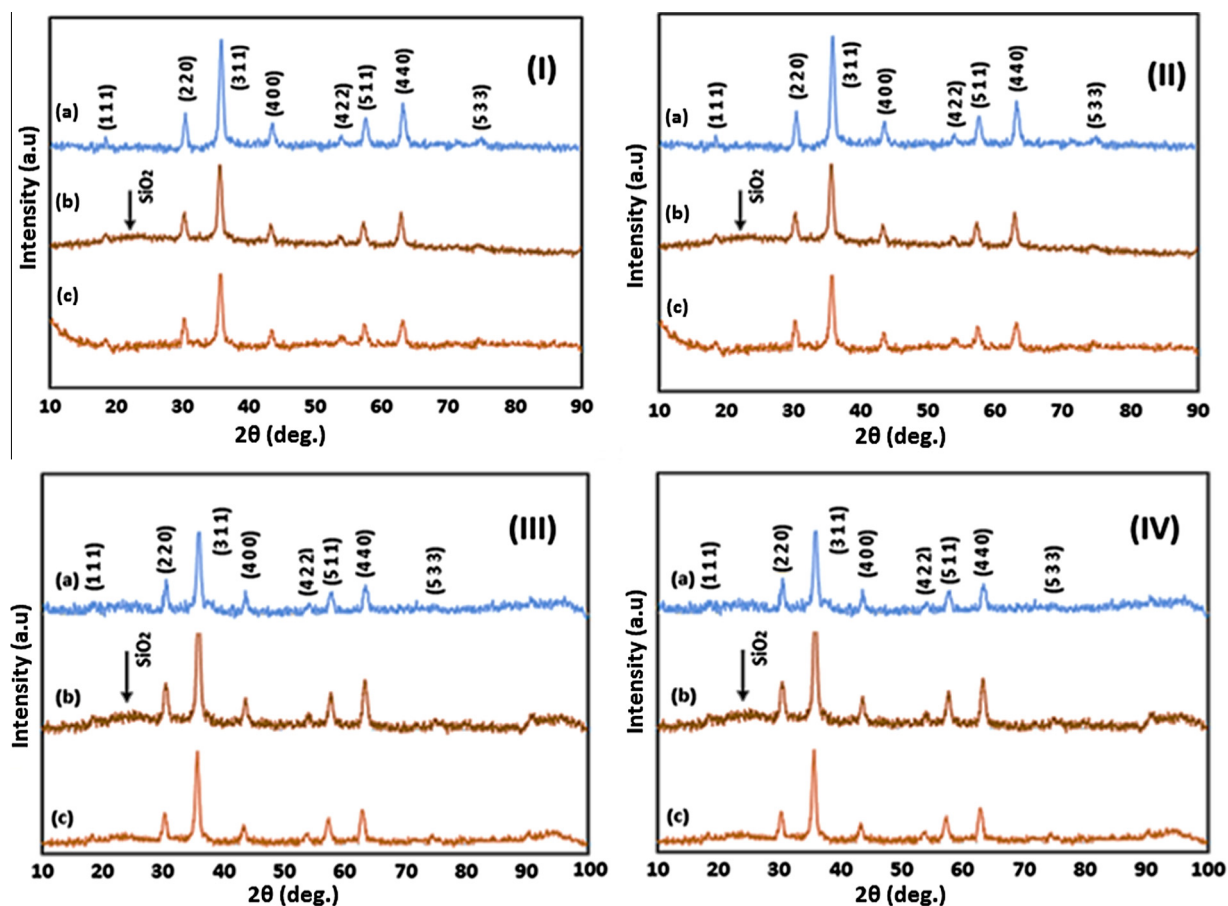


Figure 2 XRD patterns of Fe₃O₄@SiO₂ developed by incorporating Fe₃O₄ with different ratios of TEOS (I) 1:0.25, (II) 1:0.5, (III) 1:1 and (IV) 1:2. (a) Fe₃O₄@SiO₂ and (b) lipase immobilized on APTES-Fe₃O₄@SiO₂, and (c) lipase immobilized on MPTMS-Fe₃O₄@SiO₂.

values were compared with a standard curve developed using bovine serum albumin (BSA) (Bradford, 1976).

2.7. Lipase activity assay

Activity of free and immobilized lipase was measured by hydrolysis of tributyrin in an aqueous buffer solution (3 mL of 0.05 M glycine-NaOH, pH = 9.4) at 45 °C for 20 min. A known quantity of free lipase or immobilized lipase was added to the mixture and the reaction continued at the same condition. Ethanol was used to stop the reaction. The fatty acid was quantified by titration against 0.05 M sodium hydroxide. One unit (U) lipase activity is defined as the amount of lipase necessary to hydrolyze tributyrin to release 1.0 μmol of butyric acid per minute under the said assay condition.

2.8. Transesterification reaction

Transesterification was carried out in a 100 mL three necked round bottom flask kept in a water bath maintained at 45 °C. Through the central neck a slender stirrer was inserted to stir the content at 600 rpm. The second neck was used to introduce methanol. The third neck was used as a port to withdraw samples for analysis during the reaction duration. 10 mL of soybean oil, 0.5 g of immobilized catalyst and 0.43 mL of

methanol were taken in the flask. In about 20 min of the commencement of the reaction another 0.43 mL of methanol was introduced. After 20 min thereon a third dose of 0.43 mL of methanol was added. On a fixed interval 0.2 mL of the mixture was removed and analyzed for the ester content.

3. Results and discussion

3.1. Characterization of synthesized and modified magnetic nanoparticles

The FTIR spectra of Fe₃O₄@SiO₂ MNPs synthesized with different ratios of TEOS with Fe₃O₄, lipase immobilized on APTES-Fe₃O₄@SiO₂, lipase immobilized on MPTMS-Fe₃O₄@SiO₂ and pure lipase are presented in Fig. 1. The wave number of peaks in all the spectra slightly varied due to the change in quantities of TEOS on Fe₃O₄ MNPs. The wave number of SiO₂ in the Fe₃O₄@SiO₂ MNPs spectra enhanced as the TEOS component (Fe₃O₄ and TEOS ratios 1:0.25, 1:0.5, 1:1 and 1:2) increased. As the particle size increased due to the increase in surface to volume ratio decreased which necessarily reflected on the function as known from the FTIR frequencies of Fe—O (Mo et al., 1993; Khadar and George, 1992). The absorption band of Fe—O was from 561.1 to 568.9 cm⁻¹ (Fig. 1). The characteristics of all the bands slightly

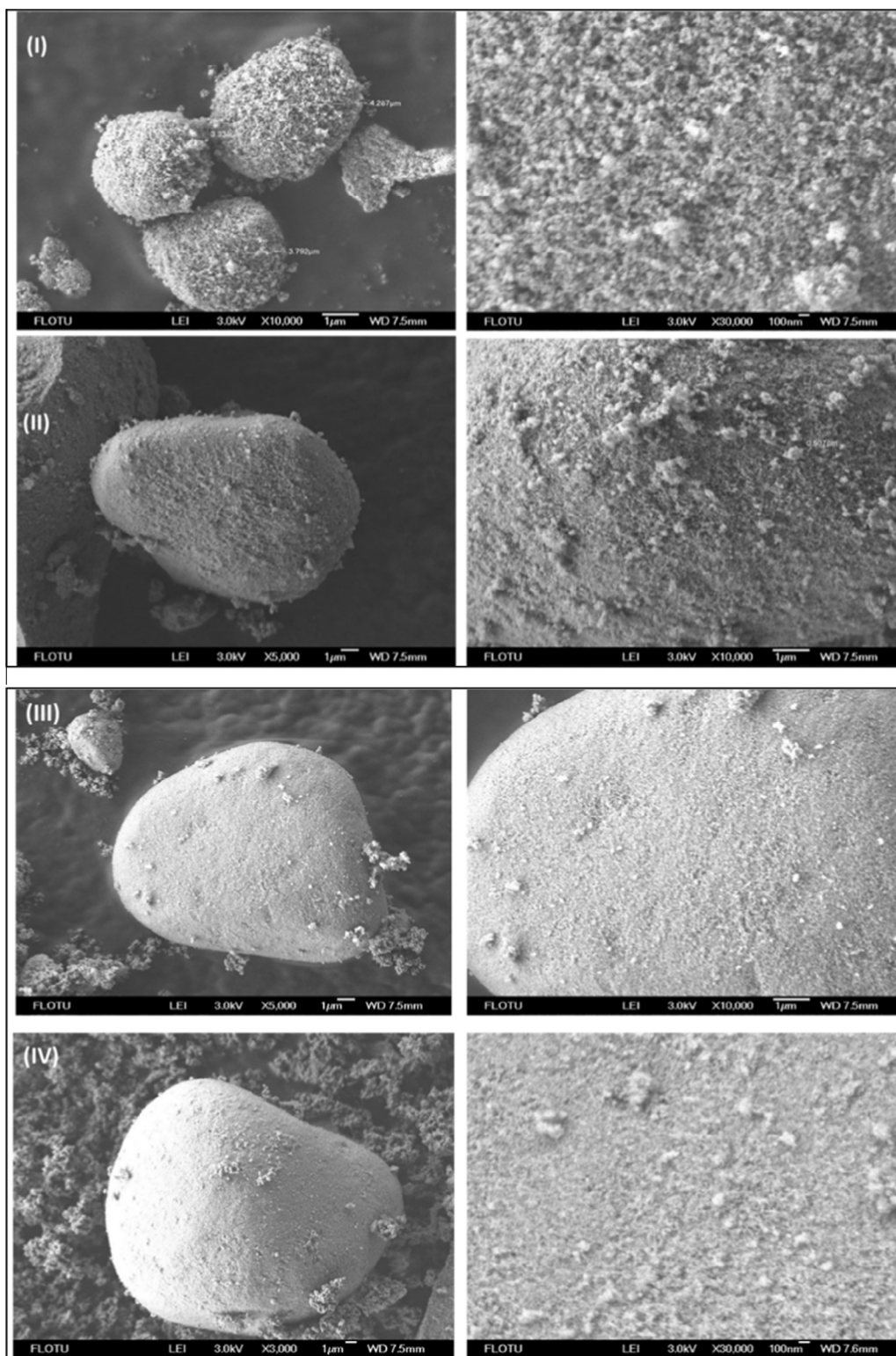


Figure 3 SEM images of $\text{Fe}_3\text{O}_4@\text{SiO}_2$ developed by incorporating Fe_3O_4 with different ratios of TEOS (I) 1:0.25, (II) 1:0.5, (III) 1:1 and (IV) 1:2.

changed while TEOS ratio was altered in the synthesis of $\text{Fe}_3\text{O}_4@\text{SiO}_2$. The wave number of $\text{Fe}_3\text{O}_4@\text{SiO}_2$ increased from 416.5 to 462.8 cm^{-1} when TEOS increased which revealed

the presence of Si—O—Si or O—Si—O bending modes. The bands at $782.5\text{--}794.5\text{ cm}^{-1}$ ascribed to the Si—O—Si symmetric stretching mode (Shen et al., 2004). The bands 1047.1--

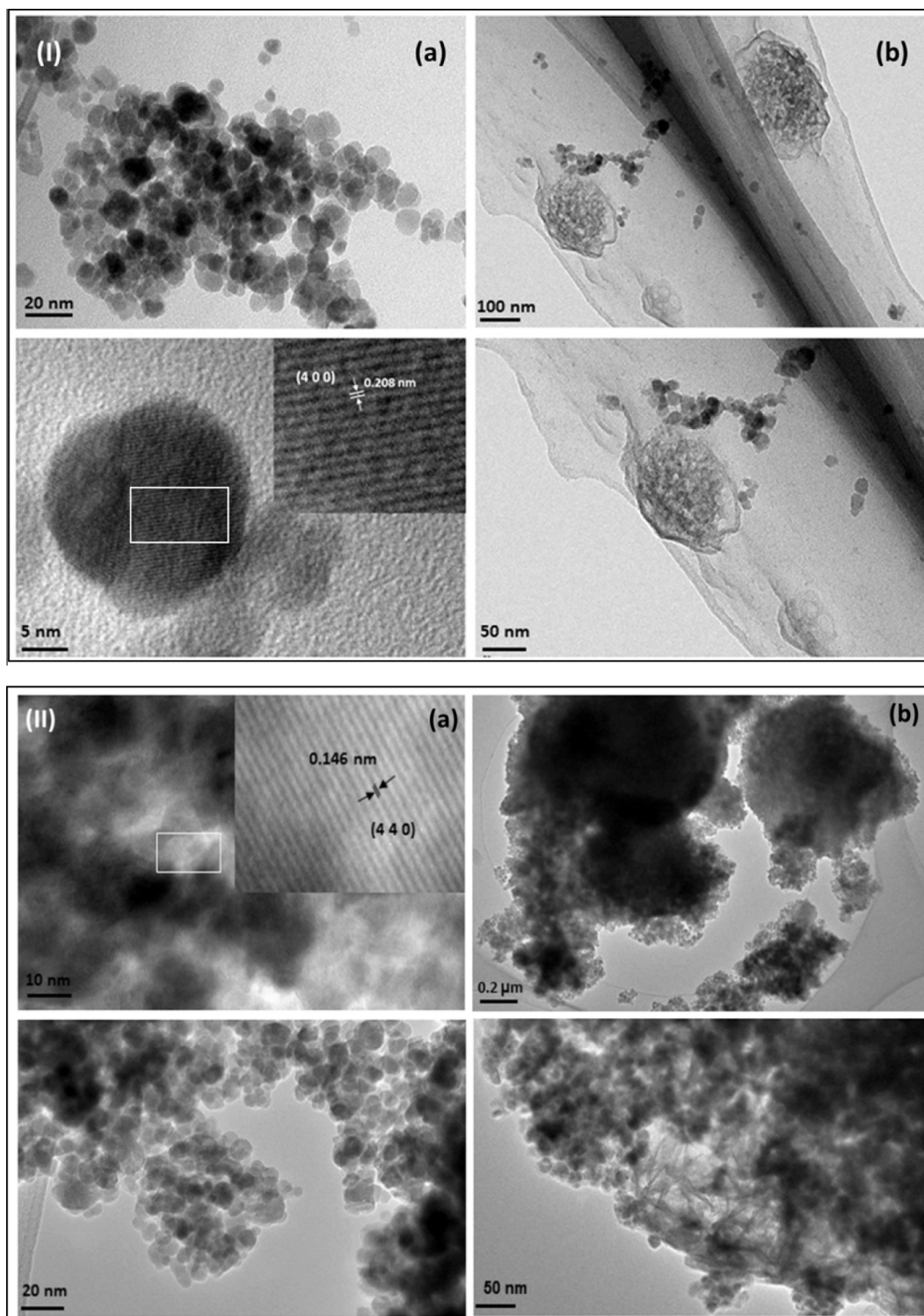


Figure 4 TEM images of Fe₃O₄@SiO₂ developed by incorporating Fe₃O₄ with different ratios of TEOS (I) 1:0.25, (II) 1:0.5, (III) 1:1, and (IV) 1:2. (a) Before lipase immobilization and (b) after lipase immobilization.

1091.5 cm⁻¹, attributed to the Si—O symmetric stretch mode due to TEOS compound. The bands 1614.1–1621.8 cm⁻¹ revealed the presence of hydroxyl groups (O—H) as the Fe₃O₄ MNPs were prepared in the aqueous phase (Bo et al., 2008). It also revealed the presence of an amino group

(N—H) (Fig. 1a). This absorption band is the reflection of the use of ammonium hydroxide in the preparation of Fe₃O₄, which might have functionalized on Fe₃O₄@SiO₂ MNPs (Wang et al., 2012). The vibration band at ~1390.1 cm⁻¹ revealed in-plane bending vibration of CH₂

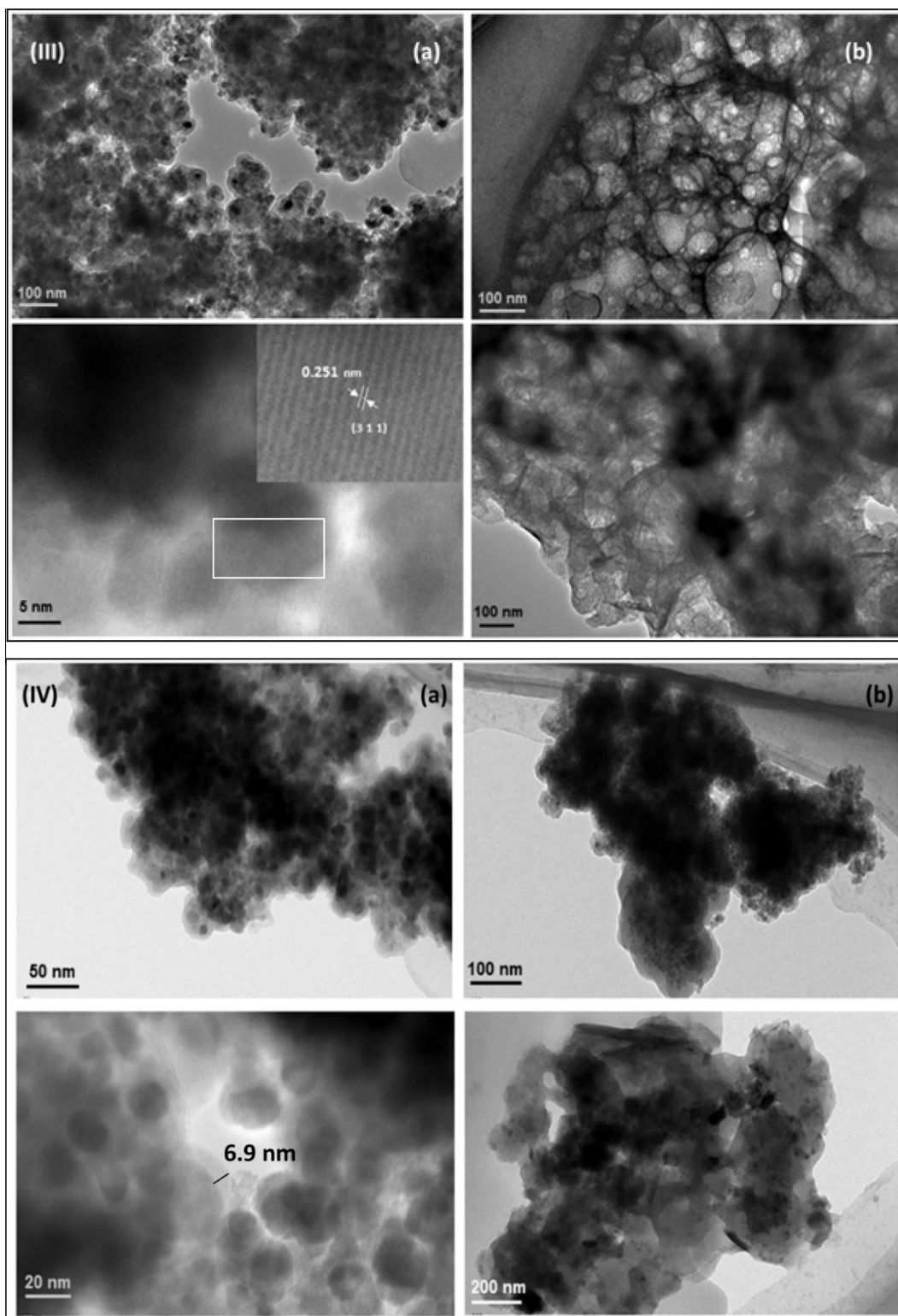


Figure 4 (continued)

which arises from the organosilane compounds (Fig. 1b and c) (Jiang et al., 2014). Lipase immobilized on the MNPs was confirmed by the variation in the FTIR spectra (Fig. 1b and c). The lipase immobilized on Fe_3O_4 MNPs clearly showed that the wave number $\sim 1641.2 \text{ cm}^{-1}$ was a bending vibration peak

of secondary amide ($\text{CO}=\text{N}-\text{H}$) (Fig. 1d and e) (Liu et al., 2005; Hong et al., 2007; Jiang et al., 2014) which was due to the lipase molecules.

The crystalline phase of the synthesized $\text{Fe}_3\text{O}_4@\text{SiO}_2$ and modified $\text{Fe}_3\text{O}_4@\text{SiO}_2$ MNPs as analyzed by XRD is shown

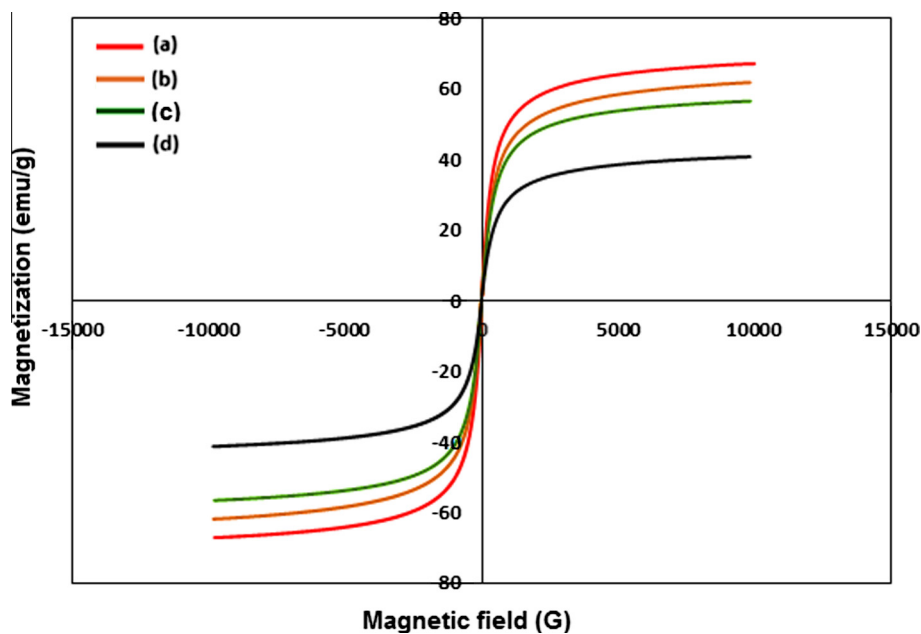


Figure 5 Magnetic behavior of Fe₃O₄@SiO₂ developed by incorporating Fe₃O₄ with different ratios of TEOS (a) 1:0.25, (b) 1:0.5, (c) 1:1 and (d) 1:2.

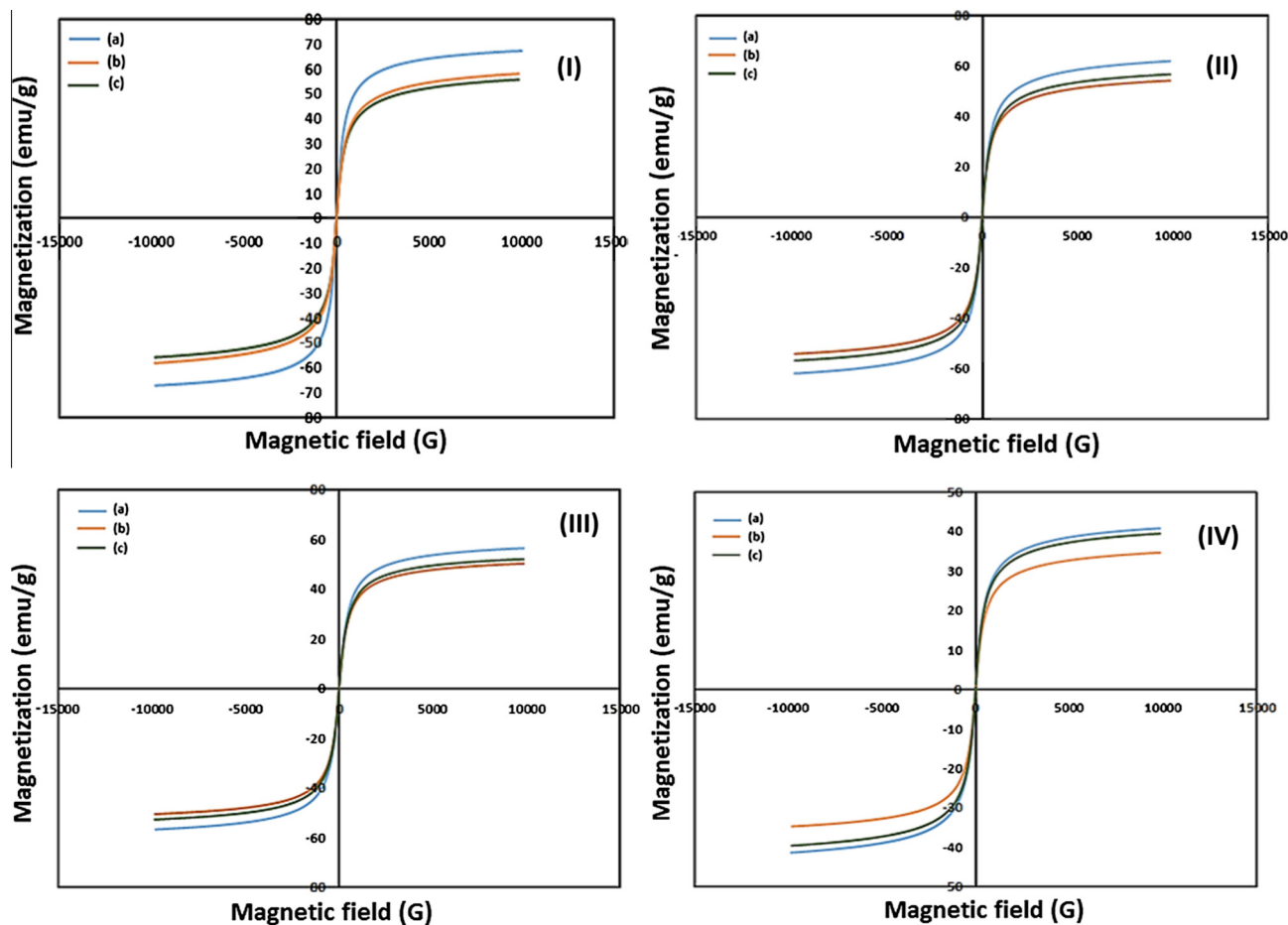


Figure 6 Magnetic behavior of lipase immobilized on Fe₃O₄@SiO₂ developed by incorporating Fe₃O₄ with different ratios of TEOS (I) 1:0.25, (II) 1:0.5, (III) 1:1 and (IV) 1:2. (a) Fe₃O₄@SiO₂, (b) lipase immobilized on APTES-Fe₃O₄@SiO₂ and (c) lipase immobilized on MPTMS-Fe₃O₄@SiO₂.

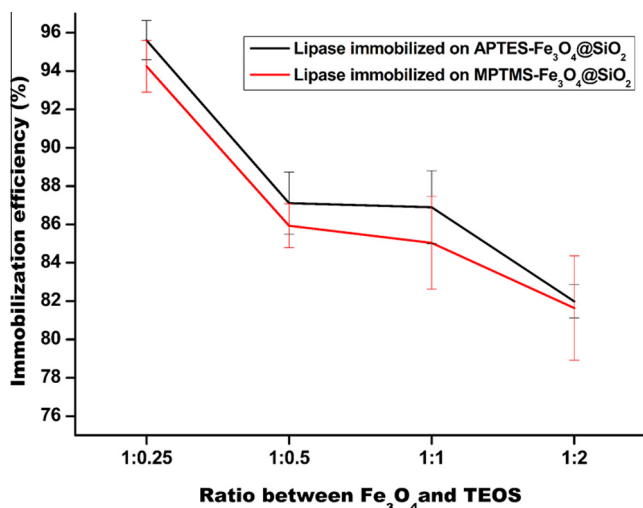


Figure 7a Immobilization efficiency of lipase immobilized on APTES-Fe₃O₄@SiO₂ and MPTMS-Fe₃O₄@SiO₂ developed by incorporating Fe₃O₄ with different ratios of TEOS. Lipase immobilization conditions: Amount of Fe₃O₄@SiO₂ 0.5 g, amount of APTES 0.3 mL, amount of MPTMS 0.6 mL, functionalization time (1 h APTES and 3 h MPTMS), glutaraldehyde concentration 10%, amount of lipase 1 mL and immobilization time 6 h.

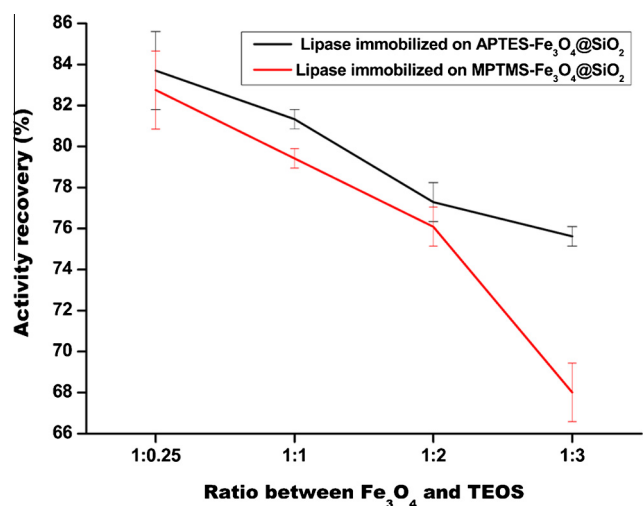


Figure 7b Activity recovery of lipase immobilized on APTES-Fe₃O₄@SiO₂ and MPTMS-Fe₃O₄@SiO₂ developed by incorporating Fe₃O₄ with different ratios of TEOS. Lipase immobilization conditions: Amount of Fe₃O₄@SiO₂ 0.5 g, amount of APTES 0.3 mL, amount of MPTMS 0.6 mL, functionalization time (1 h APTES & 3 h MPTMS), glutaraldehyde concentration 10%, amount of lipase 1 mL and immobilization time 6 h.

in Fig. 2. According to JCPDS card number 19-0629, the peaks obtained are related to Fe₃O₄ with an inverse spinel structure (Laurent et al., 2008; Zhu et al., 2015). The Fe₃O₄@SiO₂ MNPs diffraction peaks at Bragg angles 2θ ~ 18°, 30°, 35°, 43°, 53° and 57°, expressed matching with the crystal planes of (111), (220), (311), (400), (422) and (511) respectively. All the doses of TEOS with Fe₃O₄@SiO₂ MNPs more or less

Table 1 Magnetization values of Fe₃O₄@SiO₂ developed by incorporating Fe₃O₄ with different ratios of TEOS.

S. No.	Materials	Magnetization (emu/g)
(a)	1:0.25 Fe ₃ O ₄ @SiO ₂	67.16
(b)	1:0.5 Fe ₃ O ₄ @SiO ₂	61.88
(c)	1:1 Fe ₃ O ₄ @SiO ₂	56.58
(d)	1:2 Fe ₃ O ₄ @SiO ₂	41.27

indicated the same crystalline plane. Bragg peak at 22° revealed that the silica coated on Fe₃O₄ magnetic nanoparticles was in amorphous state and as a result its peak could not be observed clearly in the spectra. The XRD patterns also revealed that there were no peaks related to impurities.

SEM images of the different of Fe₃O₄@SiO₂ MNPs are presented in Fig. 3. The images indicated that the particles were agglomerated due to magnetic dipole moment between the particles. The surface of the particles greatly changed while increasing the ratio of silica coating on the Fe₃O₄ MNPs nanoparticles.

Particle size and lipase bounded on the surface of the particles as confirmed by TEM are presented in Fig. 4. The Fe₃O₄@SiO₂ (1:0.25) MNPs was of crystalline nature and its interlayer distance of d-spacing value was calculated to be around 0.208 nm (Fig. 4(I)) which represented the plane as that of (400) XRD pattern (Fig. 2). But other ratios 1:0.5 and 1:1 have d-spacing value of 0.146 and 0.251 nm which revealed the presence of other planes (440) and (311).

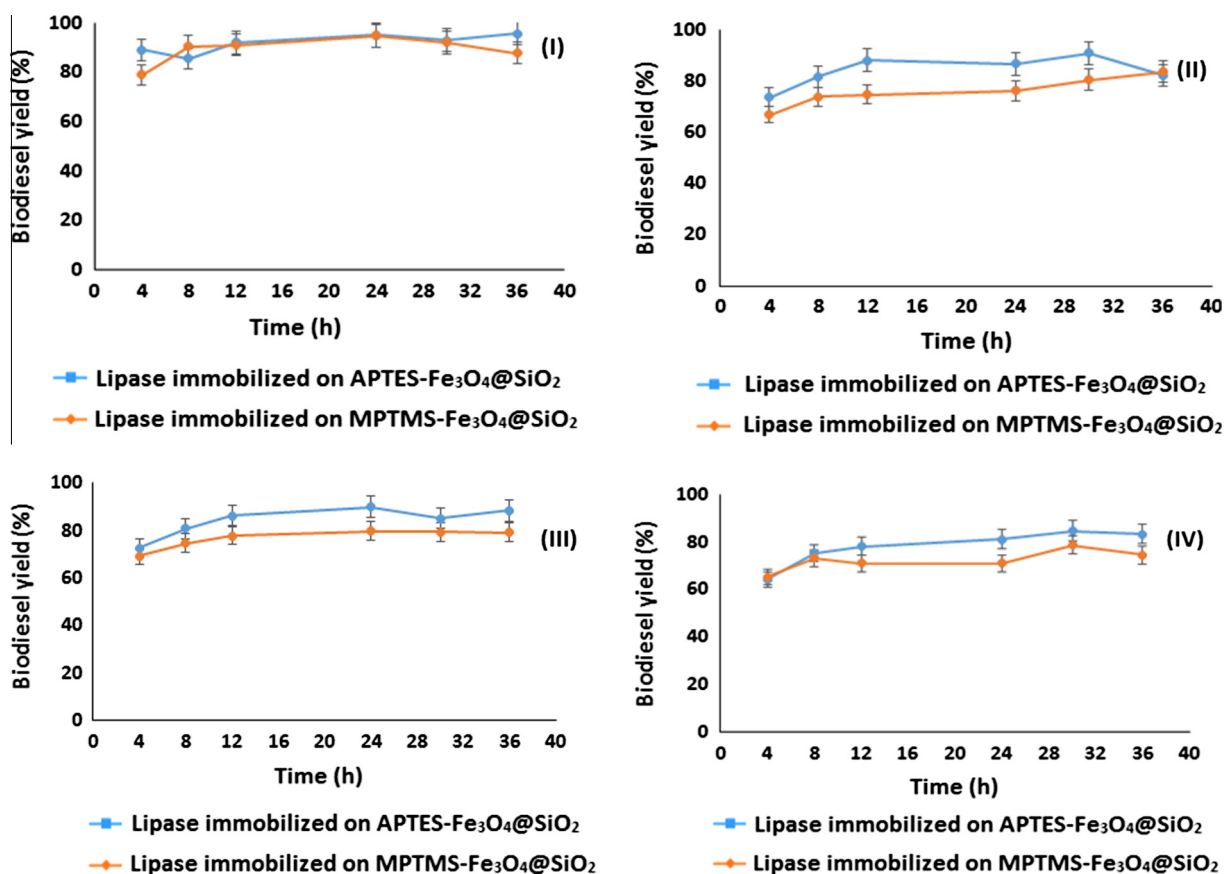
Magnetic behavior of synthesized Fe₃O₄@SiO₂ and lipase immobilized on Fe₃O₄@SiO₂ MNPs was investigated by VSM at room temperature. The saturation magnetization values for various ratios of Fe₃O₄@SiO₂ are represented in Fig. 5 and the values are given in Table 1. The synthesized silica coated Fe₃O₄ magnetic nanoparticles have superparamagnetic character due to the absence of magnetic hysteresis loops for all the samples which was an indication that both the remanence and coercivity of the samples were zero (Kumar et al., 2013). The magnetization values decreased while increasing the ratio of TEOS with Fe₃O₄@SiO₂ MNPs as silica is a diamagnetic material. Lipase immobilized on various ratios of Fe₃O₄@SiO₂ MNPs has relatively low magnetization values than that of the Fe₃O₄@SiO₂ without enzyme. Magnetization values of lipase immobilized Fe₃O₄@SiO₂ MNPs progressively decreased as the TEOS ratio enhanced in the Fe₃O₄@SiO₂ (Fig. 6 and Table 2). The saturation magnetization value of Fe₃O₄@SiO₂ MNPs with low ratios of TEOS (1:0.25) was 67.16 emu/g and the value for higher ratio (1:2) was 41.27 emu/g. Lipase immobilized on APTES-Fe₃O₄@SiO₂ MNPs had slightly higher value than the lipase immobilized on MPTMS-Fe₃O₄@SiO₂ MNPs which indicated that the support of APTES molecules on the lipase immobilization was different than MPTMS molecules. The lipase immobilized on Fe₃O₄@SiO₂ MNPs with APTES or MPTMS is having sufficient magnetization which could be useful in recovering the catalyst from the products using an external magnetic field.

3.2. Lipase immobilization efficiency and activity recovery studies by immobilized lipase

The lipase immobilization efficiency and activity recovery of immobilized lipase on the APTES-Fe₃O₄@SiO₂ and

Table 2 Magnetization values of lipase immobilized on Fe₃O₄@SiO₂ developed by incorporating Fe₃O₄ with different ratios of TEOS.

S. No	Materials name	Magnetization (emu/g)			
		1:0.25	1:0.5	1:1	1:2
1.	Lipase immobilized on APTES-Fe ₃ O ₄ @SiO ₂	55.75	54.11	50.39	34.66
2.	Lipase immobilized on MPTMS-Fe ₃ O ₄ @SiO ₂	58.07	56.69	52.50	39.51

**Figure 8** Transesterification efficiency of Fe₃O₄@SiO₂ developed by incorporating Fe₃O₄ with different ratios of TEOS and APTES or MPTMS and lipase (I) 1:0.25, (II) 1:0.5, (III) 1:1, and (IV) 1:2. Reaction conditions: soybean oil 10 mL, lipase immobilized catalyst 0.5 g, oil to methanol molar ratio 1:3, three steps: addition of methanol, temperature 45 °C and stirring rate 600 rpm.

MPTMS-Fe₃O₄@SiO₂ MNPs with different ratios of TEOS are presented in Figs. 7a and 7b. The activity recovery and immobilization efficiency reduced substantially when silica coating on Fe₃O₄ magnetic nanoparticles was increased. It was because the particle size increased due to higher dose of TEOS and consequently the lipase immobilization efficiency reduced due to the limitation in the surface to volume ratio. Impacts of particles size and immobilization conditions on enzyme activity and effectiveness thereon were investigated by immobilization of lipase and glucose oxidase in activated carbon. Enzyme loading and specific activity increased when the particles size was decreased due to a combination of three factors such as different profiles on immobilized enzyme in the porous carbon pellet, alteration of intrinsic enzyme activity due to covalent attachment to the carrier of carbon surface and effects of substrate diffusion on the observed reaction rate (Bailey and Cho, 1983). Summaries of the lipase immobiliza-

tion efficiency and activity recovery of immobilized lipase on APTES-Fe₃O₄@SiO₂ and MPTMS-Fe₃O₄@SiO₂ MNPs having different ratios of TEOS are presented in Figs. 7a and 7b. As a whole lipase immobilized on APTES-Fe₃O₄@SiO₂ achieved better activity recovery than the lipase immobilized on MPTMS-Fe₃O₄@SiO₂. In general maximum activity recovery was achieved in lipase immobilized on APTES-Fe₃O₄@SiO₂ and also on MPTMS-Fe₃O₄@SiO₂ relatively when the ratio of TEOS (1:0.25) was low. Thus this study indicated that (TEOS) the ratio of silica coating is an important factor for obtaining the maximum lipase immobilization efficiency and activity recovery.

3.3. Immobilized lipase-catalyzed biodiesel production

The transesterification trial was carried out on soybean oil using lipase immobilized on Fe₃O₄@SiO₂ MNPs with various

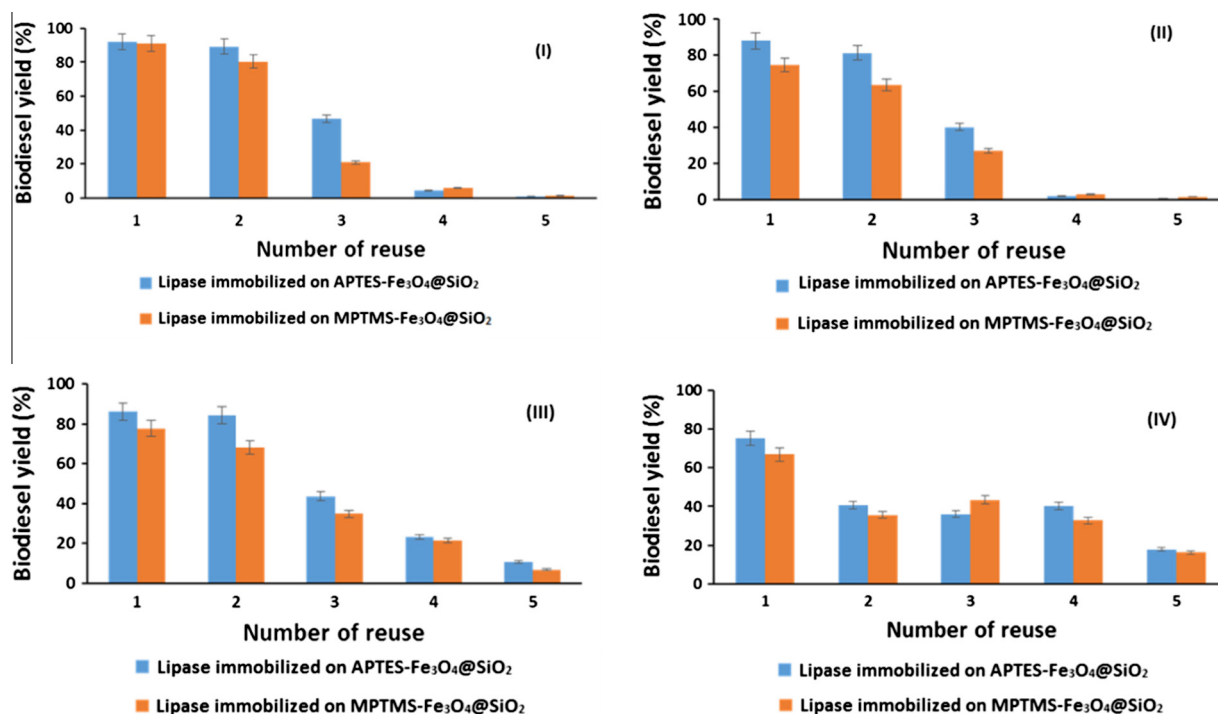


Figure 9 Reusability studies of lipase catalyst immobilized on $\text{Fe}_3\text{O}_4@\text{SiO}_2$ developed by incorporating Fe_3O_4 with different ratios of TEOS and APTES (I) 1:0.25, (II) 1:0.5, (III) 1:1, and (IV) 1:2. Reaction conditions: soybean oil 10 mL, lipase immobilized catalyst 0.5 g, oil to methanol molar ratio 1:3, three steps: addition of methanol, temperature 45°C , reaction time 12 h and stirring rate 600 rpm.

ratios of TEOS as presented in Fig. 8. The maximum yield (>90%) of fatty acid methyl esters was achieved in 8 h when $\text{Fe}_3\text{O}_4@\text{SiO}_2$ was prepared using low level of TEOS (1:0.25). Lipase immobilized on $\text{APTES-Fe}_3\text{O}_4@\text{SiO}_2$ and also on $\text{MPTMS-Fe}_3\text{O}_4@\text{SiO}_2$ expressed good catalytic ability. Yield of biodiesel above 90% as achieved in *Burkholderia* sp. lipase immobilized on $\text{Fe}_3\text{O}_4@\text{SiO}_2$ MNPs (Tran et al., 2012), *Cercospora kikuchii* lipase immobilized on rice husk (Costa-Silva et al., 2016), naturally immobilized *Carica papaya* lipase (CPL) (Su and Wei, 2014), lipase (*Schizophyllum commune* *ISTL04*) immobilized onto Celite (Singh et al., 2015) and *Candida rugosa* lipase on activated carbon (Moreno-Pirajan and Giraldo, 2011) lent great support to the present observation.

The reusability of the catalyst immobilized with lipase NS81006 was evaluated up to 5 cycles as shown in Fig. 9 and test on any additional cycle was not initiated as activity diminished in most of the catalysts in the fourth cycle itself. The catalyst reusability was not maintained well by the catalyst developed using lower ratios of TEOS (1:0.25 & 1:0.5). The higher ratio of lipase immobilized on $\text{Fe}_3\text{O}_4@\text{SiO}_2$ (1:2) enhanced the reusability than the other lower ratios. The reduction in catalytic activity while increasing the cycle is apparently due to the denaturation of the lipase and leakage of lipase from the carrier of MNPs (Yong et al., 2008). In this context, it is to be referred that the lipase (*Pseudomonas cepacia*) that was covalently immobilized on magnetic nanosilica composite particles of various structures retained its catalytic activity after five consecutive reuses (Kalantari et al., 2013). However, lipase immobilized covalently on $\text{Fe}_3\text{O}_4\text{-MCM-41}$ has retained the catalytic activity up to four cycles in the transesterification of lard and soybean oil (Xie and Zang, 2016). It

gives overall impression that this type of catalysts can be used repeatedly around four to five cycles.

4. Conclusion

Four $\text{Fe}_3\text{O}_4@\text{SiO}_2$ MNPs were developed applying different levels of TEOS which were then used in the immobilization of lipase NS81006. Increased level of TEOS causing high silica coating reduced the magnetization values, thus hampering the separation of catalyst from the reaction medium during the preparation of the biodiesel using enzyme as catalyst. APTES and MPTMS helped to increase the surface characterization of $\text{Fe}_3\text{O}_4@\text{SiO}_2$ MNPs and thereby improved the functionalization. The lipase immobilization efficiency and activity recovery reduced when the ratio of silica coating on Fe_3O_4 MNPs increased. Ester yield also reduced at higher level of incorporation of SiO_2 through TEOS on Fe_3O_4 (1:2). However the catalyst stability improved when the number of cycles increased. Lipase immobilized on $\text{Fe}_3\text{O}_4@\text{SiO}_2$ with low ratio of TEOS (1:0.25) gave high yield of esters than that of $\text{Fe}_3\text{O}_4@\text{SiO}_2$ MNPs developed with high level (1:0.5, 1:1, and 1:2) of TEOS. Lipase immobilized on $\text{APTES-Fe}_3\text{O}_4@\text{SiO}_2$ gave better performance in catalytic activity than the lipase immobilized on $\text{MPTMS-Fe}_3\text{O}_4@\text{SiO}_2$.

Acknowledgments

The authors express their gratitude to the support from Science & Technology Department of Guangdong Province (2015B020215001) and National Natural Science Foundation of China (21376139).

References

Ahangaran, F., Hassanzadeh, A., Nouri, S., 2013. *Int. Nano Lett.* 23, 1.

- Ahmadi, E., Dehghannejad, N., Hashemikia, S., 2014. *Drug Deliv.* 21, 164.
- Bae, H., Ahmad, T., Rhee, I., Chang, Y., Jin, S.U., Hong, S.J., 2012. *Nanoscale Res. Lett.* 44, 1.
- Bailey, J.E., Cho, Y.K., 1983. *Biotechnol. Bioeng.* 25, 1923.
- Bajaj, A., Lohan, P., Jha, P.N., Mehrotra, R., 2010. *J. Mol. Catal. B: Enzym.* 62, 9.
- Baskar, T., Raj, S.P., 2013. *Int. J. Sustain. Energy* 33, 525.
- Bo, Z., Min, X.J., Qi, L.Y., Zhou, L.H., 2008. *Sci. China Ser. B-Chem.* 51, 145.
- Bradford, M.M., 1976. *Anal. Biochem.* 72, 248.
- Costa-Silva, T.A., Carvalho, A.K.F., Souza, C.R.F., De Castro, H.F., Said, S., Oliveira, P., 2016. *Energy Fuels* 30, 4820.
- Fjerbaek, L., Christensen, K.V., Norddahl, B.A., 2009. *Biotechnol. Bioeng.* 102, 1298.
- Hong, J., Xu, D., Yu, J., Gong, P., Ma, H., Yao, S., 2007. *Nanotechnology* 18, 1.
- Hui, C., Shen, C., Tian, J., Bao, L., Ding, H., Li, C., Tian, Y., Shi, X., Gao, H.J., 2011. *Nanoscale* 3, 701.
- Jiang, Y., Shi, L., Huang, Y., Gao, J., Zhang, X., Zhou, L., 2014. *ACS Appl. Mater. Interfaces* 6, 2622.
- Kalantari, M., Kazemeini, M., Arpanaei, A., 2013. *Biochem. Eng. J.* 79, 267.
- Khadar, M.A., George, K.C., 1992. *Solid State Commun.* 84, 603.
- Kumar, V., Jahan, F., Raghuvanshi, S., Maharajan, R.V., Saxena, R. K., 2013. *Biotechnol. Bioprocess Eng.* 18, 787.
- Kumari, A., Mahapatra, P., Garlapati, V.K., Banerjee, R., 2009. *Biotechnol. Biofuels* 2, 1.
- Kunzmann, A., Andersson, B., Vogt, C., Feliu, N., Ye, F., Gabrielsson, S., Toprak, M.S., Buerki-Thurnherr, T., Laurent, S., Vahter, M., Krug, H., Muhammed, M., Scheynius, A., Fadeel, B., 2011. *Toxicol. Appl. Pharmacol.* 253, 81.
- Laurent, S., Forge, D., Port, M., Roch, A., Robic, C., Elst, L.V., Muller, R.N., 2008. *Chem. Rev.* 108, 2064.
- Liu, X., Guan, Y., Shen, R., Liu, H., 2005. *J. Chromatogr. B* 822, 91.
- Lu, A.H., Salabas, E.L., Schuth, F., 2007. *Angew. Chem.* 46, 1222.
- Macario, A., Giordano, G., Fromtera, P., Crea, F., Setti, L., 2008. *Catal. Lett.* 122, 43.
- Mo, C., Yun, Z., Zhang, L., Xie, C., 1993. *Nanostruct. Mater.* 2, 47.
- Morel, A., Nikitenko, S.I., Gionnet, K., Wattiaux, A., Lai-kee-him, J., Labrugere, C., Chevalier, B., Deleris, G., Petibois, C., Brisson, A., Simonoff, M., 2008. *ACS Nano* 2, 847.
- Moreno-Pirajan, J.C., Giraldo, L., 2011. *Arab. J. Chem.* 4, 55.
- Palomo, J.M., Muñoz, G., Lorente, G.F., Mateo, C., Lafuente, R.F., Guisan, J.M., 2002. *J. Mol. Catal. B: Enzym.* 19–20, 279.
- Rao, K.S., El-Hami, K., Kodaki, T., Matsushige, K., Makino, K., 2005. *J. Colloid Interface Sci.* 289, 125.
- Santra, S., Tapeç, R., Theodoropoulou, N., Dobson, J., Hebard, A., Tan, W., 2001. *Langmuir* 17, 2900.
- Serio, M.D., Tesser, R., Pengmei, L., Santacesaria, E., 2008. *Energy Fuels* 22, 207.
- Shah, S., Sharma, S., Gupta, M.N., 2004. *Energy Fuels* 18, 154.
- Shen, X.C., Fang, X.Z., Zhou, Y.H., Liang, H., 2004. *Chem. Lett.* 33, 1468.
- Singh, J., Singh, M.K., Kumar, M., Thakur, I.S., 2015. *Bioresour. Technol.* 188, 214.
- Siódmiak, T., Borowska, M.Z., Marszał, M.P., 2013. *J. Mol. Catal. B: Enzym.* 94, 7.
- Su, E., Wei, D., 2014. *J. Agric. Food Chem.* 62, 6375.
- Tao, W., Yu, P., Gong, S., Li, Q., Luo, Y., 2008. *Korean J. Chem. Eng.* 25, 998.
- Tran, D.T., Chen, C.L., Chang, J.S., 2012. *J. Biotechnol.* 158, 112.
- Wang, J., Meng, G., Tao, K., Feng, M., Zhao, X., Li, Z., Xu, H., Xia, D., 2012. *PLoS ONE* 7, 1.
- Wei, X.W., Zhu, G.X., Xia, C.J., Ye, Y., 2006. *J. Nanotech.* 17, 4307.
- Wu, W., He, Q., Jiang, C., 2008. *Nanoscale Res. Lett.* 11, 397.
- Xie, W., Ma, N., 2009. *Energy Fuels* 23, 1347.
- Xie, W., Zang, X., 2016. *Food Chem.* 194, 1283.
- Yong, Y., Bai, Y., Li, Y., Lin, L., Cui, Y., Xia, C., 2008. *J. Magn. Magn. Mater.* 320, 2350.
- Zarei, A., Amin, N.A.S., Kiakaleieh, A.T., Zain, N.A.M., 2014. *J. Taiwan Inst. Chem. Eng.* 45, 444.
- Zhu, J., Zhang, B., Tian, J., Wang, J., Chong, Y., Wang, X., Deng, Y., Tang, M., Li, Y., Ge, C., Pan, Y., Gu, H., 2015. *Nanoscale* 7, 3392.